長崎大学大学院工学研究科研究報告　第 42 巻　第 78 号　平成 24 年 1 月

An Experimental Study on Broadband Noise of a Propeller Fan

by

Soichi SASAKI*

The present research is a preliminary attempt towards the prediction of the broadband noise from the flow features, compatible with industrial constraints. In the case of low-solidity impeller, the wake rapidly expands in a wide outer part of the blades under the influence of the separation forced by the tip vortex. The broadband noise level in the low-frequency domain became large because the wake vortices with large scale in the low frequency domain were shed from the blade. Since the relative flow of the high-solidity impeller at the maximum efficiency point remains attached over the blades, the strength of vortex-shedding in the wake is reduced. Therefore the broadband noise at the maximum efficiency point is substantially decreased. At the off-design point in low flow rate, the number of blades has limited influence on the flow regime in the wake because separation likely occurs from the leading edge. In this case, the broadband noise increases with the number of blades.

Key words: *Turbo Machinery, Aerodynamic Noise, Wake, Separation*

1, Introduction

The present paper is dealing with the analysis of flow and sound measurements undertaken on low-speed propeller fans, and with preliminary predictions based on simple analytical arguments. The fans are typical of the engine cooling system. The context is the gas emission regulation Tire4 of next generation for on-engine mounted systems, which get started from 2011. In the field of construction machinery, the performance of cooling fan is requested to be improved because of the efficiency deterioration of the heat exhaust caused by the regulation. Therefore, it is necessary to generate a large amount of artificial wind for the engine cooling since the machine cannot expect benefit from the wind due to the advancing speed as an automobile. Increasing the needed flow rate of the fan leads to an increase in the associated noise. Moreover, in order to balance the resistance brought by the radiator and the engine, the operation point of the cooling fan is shifted to a so-called off-design point lower than the maximum efficiency point.

In the context of engine cooling, the blade-tip Mach number of the propeller fans is usually small. The background of the acoustic analogy states that the fan noise sources reduce to lift fluctuations on the blades, acting as equivalent dipoles. In these conditions, the intensity of the aerodynamic sound scales with the fifth or sixth power of a characteristic flow velocity. The noise itself is the sum of a series of tones at the harmonics of the blade passing frequency, caused by the periodic interactions, and of broadband noise arising from turbulence in the flow. The present study is focused on broadband noise.

Sharland first derived a prediction equation of the broadband noise generated from an axial fan based on the acoustic analogy [1]. Fukano *et al*. made further improvements to the theory. According to their statement, the noise generated from a low-pressure axial-flow fan can be related to the wake characteristics. Some impeller noise predictions were made with high accuracy on this background, addressing simple fan architectures [2-4]. The authors previously performed experimental studies on the aerodynamic characteristics and the noise of a ring fan, as an improved alternative to classical propeller fans [5-6].

Received Dec. 14, 2011

* Assistant Professor, Department of System Science

The ring fan is a propeller fan on which a ring-shape shroud is added at the blade tip side [7]. It is expected not only to improve the flow around the tip but also to increase the rigidity of the impeller. It has already been pointed out experimentally that the ring fan not only improves the efficiency by approximately 12 % but can also decrease the fan noise at the maximum efficiency point by around 3 dB. Apart from these previous efforts, it is still necessary to improve the design of efficient impeller fans and to provide guidelines for the choice of key parameters such as the number of blades. Furthermore there is a real need of clarifying the relationships between the main flow features and the associated noise.

The present research is a preliminary attempt towards the prediction of the broadband noise from a minimal knowledge of the flow features, compatible with industrial constraints. The aerodynamic characteristics, the noise spectrum and wake parameters of propeller fans having different number of blades are measured. The broadband noise of the propeller fans is analyzed and predicted based on the wake characteristics measured in a downstream stationary coordinate system. The operation point is set both at the maximum efficiency flow rate and a off-design point of lower flow rate.

2, Experimental Setup

Figure 1 shows pictures of the investigated impellers, the main dimensions of which are listed in table 1. A part of the shape of the blade section is shown in Fig. 2. The chord length of the tip side is 122 mm and the hub side is 66 mm. The blade design is the same and only the number of blades is varied. The hub ratio ($\nu = D_{hub}/D$) is 0.424. In the following, the impellers with 7, 14 and 21 blades are referred to as P7, P14 and P21, respectively.

A schematic view of the experimental setup is shown in Fig. 3. The height and width of the duct are 1 m each, while its total length is about 4 m. The dynamic pressure is measured 600 mm upstream of the impeller disc using a Pitot tube. The flow rate is deduced from the dynamic pressure. It is controlled by an adjustable throttle at the duct exit. The static pressure of the fan is measured 400 mm upstream from the exit. The rotational speed of the driving shaft is 1200 rpm. The shaft torque of the motor is measured using a torque meter (Ono-Sokki; SS-500); the efficiency of the fan can be estimated on the basis of the ratio of shaft power to theoretical power. The flow

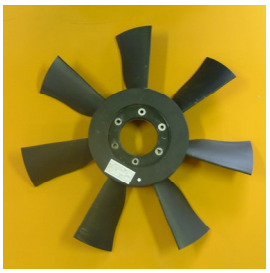

(a) P7

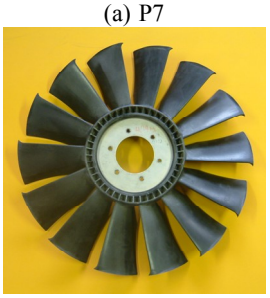

(b) P14

(c) P21

Fig. 1 Test impeller

Table 1 Main dimensions

Impeller	P7	P14	P21
C (mm)	122		
C_{hub} (mm)	66		
D (mm)	613		
D_{hub} (mm)	260		
$\nu = D_{hub}/D$	0.424		
t (mm)	3		
Z	7	14	21

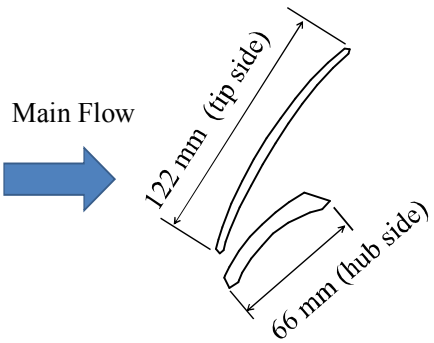

Fig. 2 Shape of the blade section

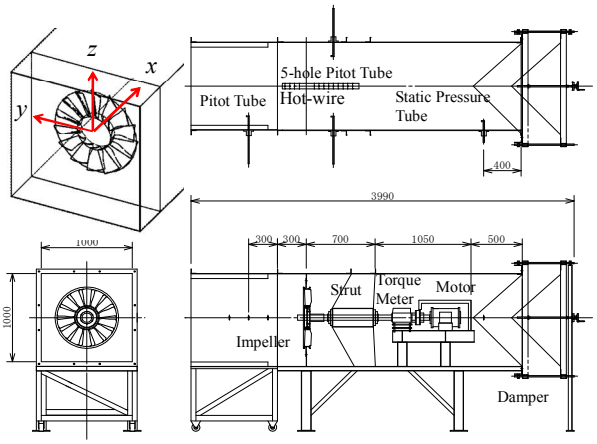

Fig. 3 Experimental apparatus

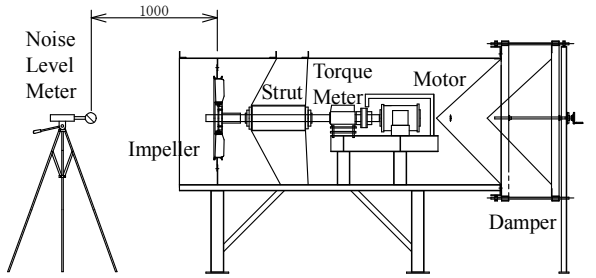

Fig. 4 Fan noise measurement setup.

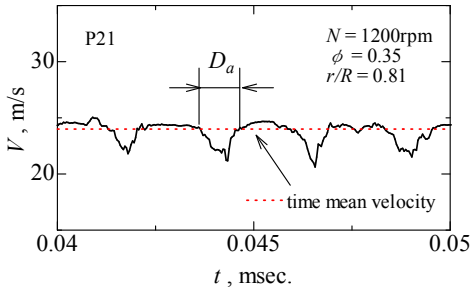

Fig. 5 The velocity fluctuation measured by the hot-wire anemometer

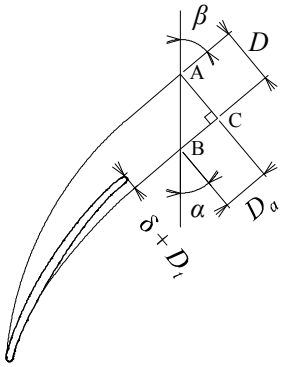

Fig. 6 The width of wake in relative coordinate system

coefficient φ, the static pressure coefficient ψ_s, the power coefficient λ and the efficiency η are summarized below as

$$\phi = \frac{Q}{60\,\pi\,D\,b\,U}, \psi_s = \frac{2\,P_s}{\rho\,U^2}$$
$$\lambda = \frac{2\,L}{\rho\,\pi\,D\,b\,U^3}, \eta = \frac{\varphi\,\psi}{\lambda} \qquad (1)$$

The flow in the fan wake is characterized using a hot-wire anemometer system (KANOMAX JAPAN, Inc.) and a 5-holes Pitot tube. The experimental setup for fan noise measurements is shown in Fig. 4. A 1/2-inch microphone (ONO-SOKKI; LA-4350) is set at a distance of 1.0 m from the impeller inlet, on the axis. The frequency content of the delivered signal is provided by a FFT analyzer, with a bandwidth of 25 Hz.

3, Fan Noise Prediction Theory

Fukano *et al.* [2] proposed a prediction equation for the sound power generated from a fan as

$$E = \frac{\pi\,B\,\rho}{2400\,a_0^{\,3}} \int_{SPAN} DW^6 dz \qquad (2)$$

where B is the number of blades, ρ is the density of the air, D is the wake width, W is the relative velocity, z is the span-wise coordinate and a_0 is the speed of sound. In reference [2], the relative velocity has been defined by the inlet velocity. The relation between the sound power and sound pressure at the measurement point is defined as

$$\frac{E}{2} = \frac{4\,\pi\,R^2}{3\,\rho\,a_0\,\cos^2\theta}\,\overline{p^2} \qquad (3)$$

where R is the distance between the noise source and the observation point (R = 1.0 m), θ is the angle that expresses the directivity of the sound (θ = 0°). This is justified by the property that self-noise from an axial fan is not blade-to-blade correlated and radiates dominantly on axis. The sound pressure level is defined by

$$L_p = 10\log\left(\frac{\overline{p^2}}{p_o^{\,2}}\right) \qquad (4)$$

where p_0 is the reference sound pressure (20μPa).

Typical velocity fluctuations measured by the hot-wire anemometer in the wake are plotted in Fig. 5. The I-type hot-wire probe (KANOMAX; 0251R-T5), which inclined to the absolute flow angle measured by the 5-hole Pitot tube, is set up to the experimental apparatus. Using the

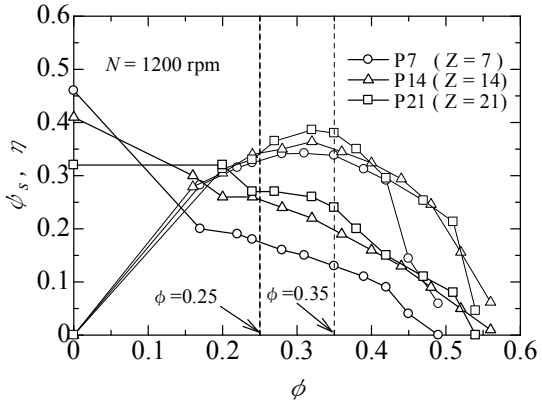

Fig. 7 Aerodynamic characteristics

circumferential velocity at the measurement position, the time scale can be changed for a length scale to evaluate the wake width. The wake widths measured in the absolute coordinate system and the relative coordinate system are related according to Fig. 6. The wake center line is assumed to be parallel to the stream line at relative flow angle β, so that the wake width measured in the absolute coordinate system becomes D_a. The wake width in the relative coordinates is given by the line from A to C.

4, Results and Discussion

The aerodynamic characteristics of the propeller fans are shown in Fig. 7. The static pressure coefficient of the P21 is the highest over a wide range of flow rates. Accordingly, the efficiency of P21 in the vicinity of the maximum efficiency point (φ=0.35) is the highest. The broadband noise is analyzed in detail around the off-design point (φ=0.25) in the low flow rate domain and at the maximum efficiency point (φ=0.35).

The sound pressure level spectra of the three fans are compared in Fig. 8. At the maximum efficiency point, the tonal noise at the blade passing frequency and the harmonics is dominant. The broadband noise in the range 100 Hz to 300 Hz for P21 is lower than that of P7 and P14. It is worth noting that according to A-weighted noise levels, frequencies below 100 Hz are negligible. Therefore, at off-design point in Fig. 8 (b), the broadband noise level distributed from 100 Hz to 500 Hz becomes dominant. Moreover, at both operation points, the broadband noise above 1000Hz is almost the same for all fans, except for the slightly higher level of P21 in Fig.8 (b).

The noise characteristics of the propeller fans are shown

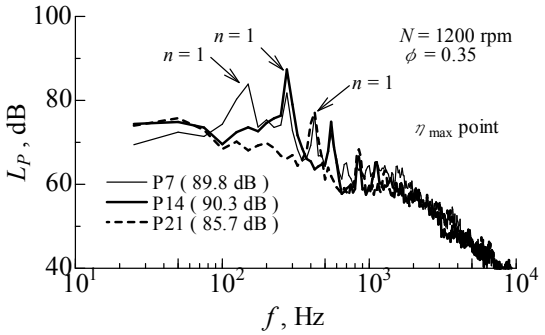

(a) maximum efficiency point (ϕ =0.35)

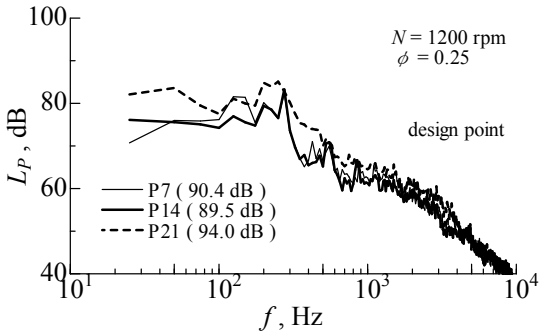

(b) off-design point (ϕ =0.25)

Fig. 8 Sound pressure level spectra of the tested fans

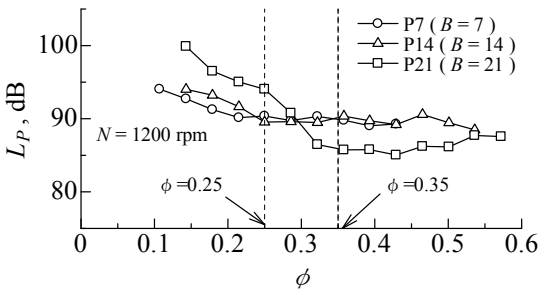

(a) Overall noise level

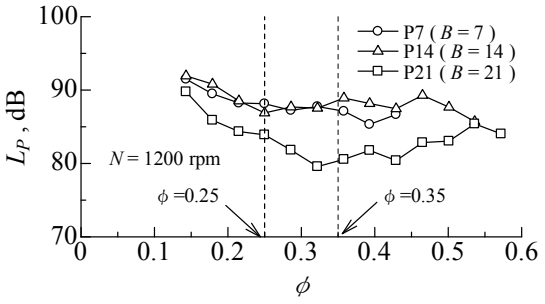

(b) Discrete frequency noise level (n=1)

Fig. 9 Noise characteristics

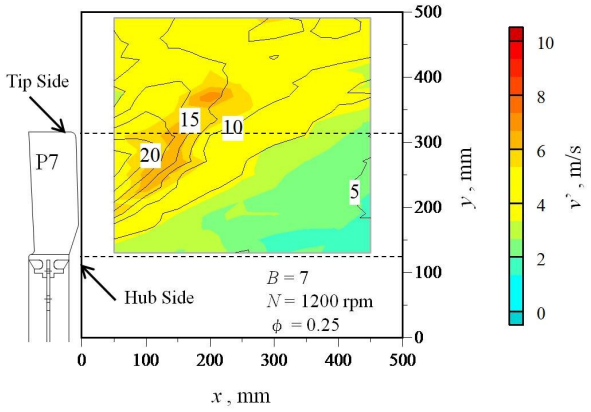

(a) P7 (off-design point)

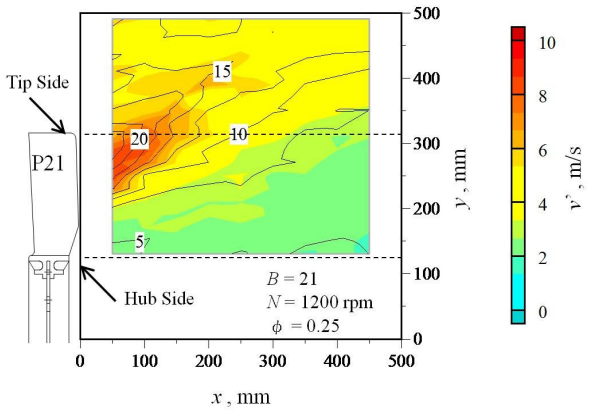

(b) P21 (off-design point)

Fig. 10 Flow field at the off-design point measured by the hot-wire probe (φ=0.25)

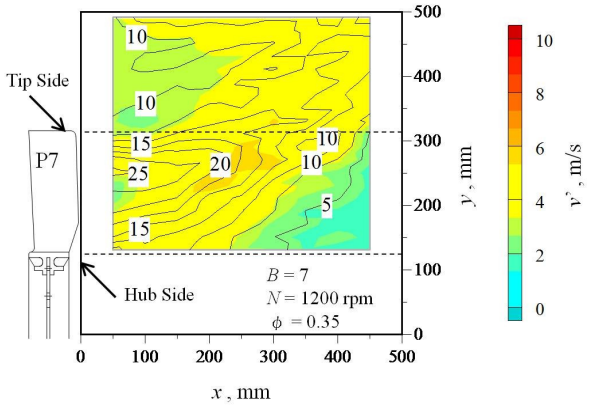

(a) P7 (maximum efficiency point)

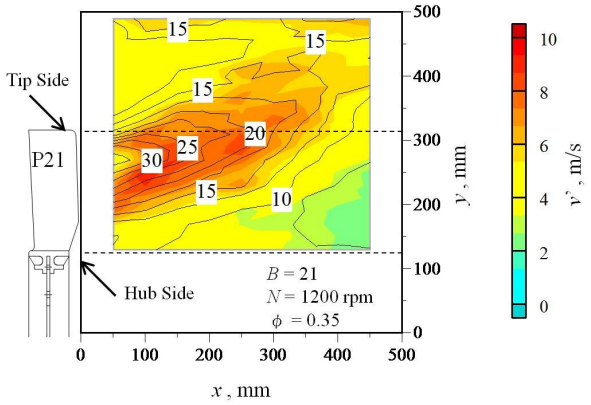

(b) P21 (maximum efficiency point)

Fig.11 Flow field at the maximum efficiency point measured by the hot-wire probe(φ=0.35)

in Fig. 9. Figure 9 (a) reports about the overall noise level and Fig. 9 (b) about the tonal noise cumulated on the first harmonics. In the case of maximum efficiency point, the overall noise and the tonal noise follow the same trend. This indicates that the former dominates. In contrast, the tonal noise behavior of P21 departs from the overall noise level at the off-design point (φ=0.25). At this point and for this fan, it is considered that the broadband noise dominates. Globally noise reduction strategies have to focus on broadband noise in the present application.

In Fig. 10, the flow field in the meridian plane is presented. The operation point is the off-design point (φ=0.25). Figure 10 (a) addresses the P7, and Fig.10 (b) the P21. The lines stand for the mean velocity iso-contours and the amplitude of the velocity fluctuations is superimposed as a color map. In both figures, the main working area of the propeller fan, forms in the span range 200 mm < r < 300 mm. The velocity fluctuations reach their maximum amplitude in the velocity gradients. Therefore, it is considered that the aeroacoustic sources are likely to onset on the blade surface in the upstream continuation of the location of large fluctuating intensity. At the off- design point, the velocity fluctuations in the wake of P21 are much higher than that of P7. The intensity of the velocity fluctuation follows the same trend with the noise characteristics of the fan at the maximum efficiency point (see Fig. 9). The flow field at the maximum efficiency point is shown in Fig. 11. In the case of P21 in Fig.11 (b), the intensity of the velocity fluctuation not only at the hub side but also at the tip side becomes large at the velocity gradient. In this case, the intensity of velocity fluctuations does not correlate as well with the fan noise.

The span-wise distributions of wake width are given in Fig. 12. The measurement point was chosen 30 mm downstream from the trailing-edge section of the fan. It is suitable to estimate for the wake characteristics at the vicinity of 1D (in this case; 30 mm) because the dead air region is formed within the 1D wake domain. For instance,

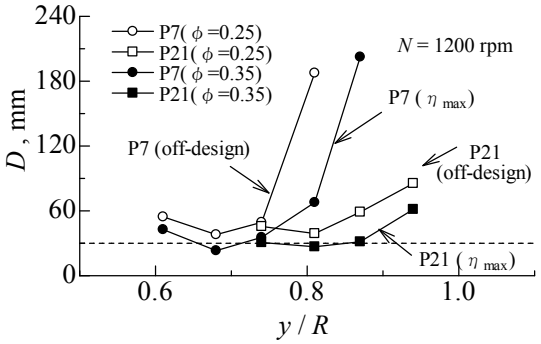

Fig. 12 Span-wise distribution of the wake width scaled by the rotor pitch

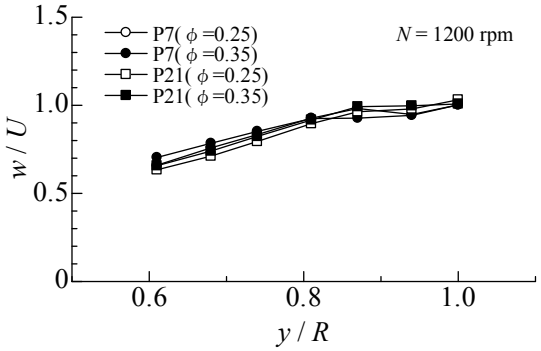

Fig. 13 Span-wise distribution of the relative velocity

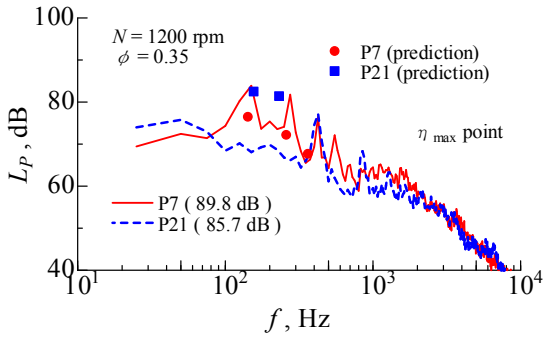

(a) maximum-efficiency point (ϕ =0.35)

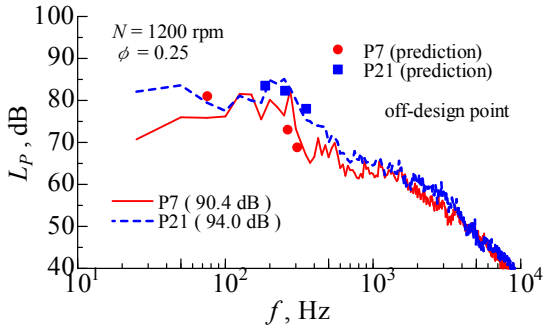

(b) off-design point (ϕ =0.25)

Fig. 14 Comparison of low-frequency predicted noise levels with measured noise spectra

the width of the wake of P7 increases rapidly from r/R=0.74 because of the roll-up of a tip vortex, whereas the wake of P21 gradually develops from r/R=0.81. It is considered that the tip vortex is hard to form at the blade tip side because of narrow blade pitch in P21. The wake width at the maximum efficiency point is smaller than at the off-design point since the relative flow is along the blade. The span-wise distribution of the relative velocity is shown in Fig. 13. For the relative flow, it is assumed that the wake vortex is formed by leading-edge separation according to the principle of Fukano's prediction theory. The normalized relative velocities by the circumferential velocity distribute almost same.

The predicted noise levels according to Fukano's model are superimposed on the measured spectra in Fig. 14. At the maximum efficiency point, the predicted noise level of P7 agrees well to the measured noise level, whereas the predicted noise level of P21 becomes larger than the measured broadband noise level. The intensity of velocity fluctuations did not correlate as well with the fan noise in this case of P21 (see Fig. 11 (b)). Therefore, it is considered that the wake vortex does not shed no longer from the blade in the case of maximum efficiency point of P21 because of the increased number of blades. In contrast at the off-design point, the broadband noise level of P21 exceeds that of P7. The relative velocities used in the model predictions do not differ a lot for this operation point, whereas the wake width in the case of off-design point becomes large than the maximum efficiency point. Therefore, it is concluded that the increase of blade number and the separated flow are responsible for the higher broadband noise of P21.

5, Conclusions

(1) In the case of low-solidity impeller P7, the wake rapidly expands in a wide outer part of the blades under the influence of the separation forced by the tip vortex. The broadband noise level in the

low-frequency domain became large because the wake vortices with large scale in the low frequency domain were shed from the blade.

(2) Since the relative flow of the high-solidity impeller P21 at the maximum efficiency point remains attached over the blades, the strength of vortex-shedding in the wake is reduced. Therefore the broadband noise at the maximum efficiency point is substantially decreased.

(3) At the off-design point in low flow rate, the number of blades has limited influence on the flow regime in the wake because separation likely occurs from the leading edge. In this case, the broadband noise increases with the number of blades.

References

[1] I. J. Sharland, 1964, Sources of Noise in Axial Flow Fans, *Journal of Sound Vibration*, 1-3, pp.302–322.

[2] Fukano, T., Kodama, Y., Senoo, Y., 1977, Noise generated by low pressure axial flow fans, I: Modeling of the turbulent noise, *Journal of Sound and Vibration*, 50(1), pp. 63-74.

[3] Fukano, T., Kodama, Y., Takamatsu, Y., 1977, Noise generated by low pressure axial flow fans, II: Effects of number of blades, chord length and camber of blade, *Journal of Sound and Vibration*, 50(1), pp. 75-88.

[4] Fukano, T., Kodama, Y., Takamatsu, Y., 1978, Noise generated by low pressure axial flow fans, III: Effects of rotational frequency, blade thickness and outer blade profile, *Journal of Sound and Vibration*, 56(2), pp. 261-277.

[5] Sasaki, S., Fukuda, M., Tsubota, H., Tsujino M., 2010, Influence of Internal Flow on Aerodynamic Characteristics of a Ring Fan, *Turbomachinery* (in Japanese), 38(12), pp. 729-736.

[6] Sasaki, S., Fukuda, M., Tsujino, M., Tsubota, H., 2011, Prediction of Aerodynamic Noise in a Ring Fan Based on Wake Characteristics, *Journal of Thermal Science*, 20(2), pp. 144-149

[7] R.E. Longhouse, 1978, Control of tip-vortex noise of axial flow fans by rotating shrouds, *Journal of Sound and Vibsration*, 58(2), pp. 201- 214.